Structural Changes Accompanying GTP Hydrolysis in Microtubules: Information from a Slowly Hydrolyzable Analogue Guanylyl-(α,β)-Methylene-Diphosphonate

Anthony A. Hyman,* Denis Chrétien,* Isabelle Arnal,‡ and Richard H. Wade‡

*Cell Biology Program, European Molecular Biology Laboratory, Heidelberg 69012, Germany; and ‡Laboratoire de Microscopie Electronique Structurale, Institut de Biologie Structurale Jean Pierre Ebel (CEA-CNRS), 38041 Grenoble Cedex 1, France

Abstract. We have used cryoelectron microscopy to try to understand the structural basis for the role of GTP hydrolysis in destabilizing the microtubule lattice. We have measured a structural difference introduced into microtubules by replacing GTP with guanylyl-(α,β)-methylene-diphosphonate (GMPCPP). In a stable GMPCPP microtubule lattice, the moiré patterns change and the tubulin subunits increase in size by 1.5 Å. This information provides a clue to the role of hydrolysis in inducing the structural change at the end of a microtubule during the transition from a growing to a shrinking phase.

MICROTUBULES are polymers of the tubulin heterodimer involved in such diverse functions as the regulation of membrane traffic and chromosome separation during mitosis. They consist of protofilaments, head to tail alignments of the tubulin α–β heterodimer (Amos and Klug, 1974; Kirschner, 1978; Purich and Kristoffersen, 1984) that run lengthwise along the microtubule axis and interact through lateral contacts to form the microtubule wall. Microtubules exist in dynamic equilibrium with tubulin subunits, growing and shrinking by addition or loss of tubulin dimers from the ends of the protofilaments. Growth is governed by the concentration-dependent on-rate of tubulin subunits, but the shrinking rate is extremely rapid and independent of the tubulin concentration. Individual microtubules switch stochastically between phases of slow growth and fast shrinkage so that in a microtubule population, some will be growing and some shrinking, a property known as dynamic instability (Cassimeris et al., 1988; Gelfand and Bershadsky, 1991; Mitchison and Kirschner, 1984; Walker et al., 1988).

Dynamic instability is a highly nonequilibrium behavior, and the energy source that drives the nonequilibrium state is GTP hydrolysis. The tubulin dimer has one exchangeable GTP site (E site) on the β subunit that must be occupied by GTP to allow the dimer to participate in microtubule assembly. The polymerization rate is controlled by the binding constant of GTP tubulin for the microtubule ends but, during or after polymerization, GTP is hydrolyzed to GDP that is trapped in the lattice in the form of tubulin-GDP (Carlier, 1989; Kirschner, 1978; Purich and Kristoffersen, 1984). Experiments using GTP analogues have shown that GTP hydrolysis is not required for microtubule growth, but is necessary for microtubules to be able to shrink (Hyman et al., 1992; Mejillano et al., 1990; Penningroth and Kirschner, 1978; Seckler et al., 1990). The most common model to explain the role of GTP hydrolysis suggests that the end of the microtubule is capped by subunits with unhydrolyzed GTP so as to stabilize the microtubule against depolymerization. Loss of this cap stimulates shrinkage (Carlier, 1989; Chen and Hill, 1985; Kirschner and Mitchison, 1986; Mitchison and Kirschner, 1984). To date, however, it has not been possible to detect any unhydrolyzed GTP in microtubules, suggesting that the cap must be either very small or nonexistent (Erickson and O'Brien, 1992; O'Brien et al., 1987; Stewart et al., 1990).

Structural analysis of microtubules suggests that interactions between protofilaments are an essential feature regulating the transitions between growing and shrinking phases. Microtubules appear to grow as a sheet of interacting protofilaments that later close into a tube (Erickson, 1974; Simon and Salmon, 1990; Chrétien, D., S. Fuller, and E. Karsenti, manuscript submitted for publication). When microtubules shrink, the protofilaments loose their contacts, curl out from the microtubule ends, and then they appear to break off as tubulin oligomers (Mandelkow et al., 1991; Simon and Salmon, 1990). We wished to find out whether GTP hydrolysis changed the stability of microtubules by modulating microtubule structure. To investigate this problem, we took advantage of guanylyl-(α,β)-methylene-diphosphonate (GMPCPP)[1], a nonhydrolyzable analogue of GTP.

Address all correspondence to Anthony A. Hyman, Cell Biology Program, European Molecular Biology Laboratory, Meyerhofstrasse 1, Heidelberg 69012, Germany. Tel.: (49) 6221-387-338. Fax: (49) 6221-387-306.

1. *Abbreviation used in this paper*: GMPCPP, guanylyl-(α,β)-methylene-diphosphonate.

Microtubules polymerized in the presence of GMPCPP are stable, presumably because this analogue mimics the unhydrolyzed form of GTP in the microtubule surface lattice (Hyman et al., 1992). It might, therefore, be that analysis of the structure of a GMPCPP lattice would give a clue about the structure of a GTP lattice, for instance, structural motifs that reveal a cap of GTP subunits at the end of the microtubule. The advantage of GMPCPP compared to other GTP analogues is that it competes well with GTP for the tubulin nucleotide-binding site, and it mimics the growth rate of microtubules from GTP tubulin, but it completely stabilizes microtubules against depolymerization (Hyman et al., 1992). Using electron cryomicroscopy, we have compared the structure of microtubules assembled from GTP-tubulin, which we will call GDP microtubules, with those assembled from GMPCPP tubulin, which we will call GMPCPP microtubules. We have found differences between the two types of microtubules, suggesting that there could be a structural basis for the role of GTP hydrolysis in dynamic instability.

Materials and Methods

Tubulin was purified by the method of Weingarten et al. (1975) with modifications by Mitchison and Kirschner (1984). After the phosphocellulose column, it was purified by a further polymerization/depolymerization cycle, frozen in liquid nitrogen, and stored as 50-μl aliquots at −80°C. (Hyman et al., 1991). Rhodamine tubulin was prepared as in Hyman et al. (1991). Before use, tubulin was thawed and spun at 13,000 *g* for 15 min. GMPCPP was synthesized as described in Hyman et al. (1992). All other chemicals were from Sigma Immunochemicals (St. Louis, MO).

Assembly

To assemble microtubules, tubulin was thawed and spun for 15 min at 15,000 *g* at 4°C. To examine microtubules by fluorescence microscopy, 1 part of rhodamine tubulin was added to 10 parts of underivatized tubulin and assembly monitored using a fluorescence microscope (Howard and Hyman, 1993). To examine GDP microtubules polymerized by self assembly, tubulin was diluted to 5 mg/ml in BRB80 + 1 mM GTP on ice and warmed to 37°C. To polymerize GMPCPP microtubules, tubulin was diluted to 0.4 mg/ml in BRB80 + 1 mM GMPCPP on ice and polymerized for 1 h at 37°C. To construct mixed microtubules, GMPCPP microtubules were assembled at 0.3 mg/ml + 100 μM GMPCPP with no rhodamine tubulin for 15 min. These GMPCPP microtubules were diluted 1:1 in the presence of 5 mg/ml tubulin supplemented with 0.5 mg/ml rhodamine tubulin + 1 mM GTP to give a final GTP tubulin concentration of ~3 mg/ml. Growth continued for 3 min before examination. The two fluorescent GTP ends were separated by a nonfluorescent GMPCPP segment, but the two fluorescent segments could easily be seen to belong to the same microtubule by their movement characteristics in solution. The total length of these segmented microtubules was ~10 μm. Under these conditions, GMPCPP microtubules had a site occupancy of 0.65 (Hyman et al., 1992).

Electron Cryomicroscopy

Microtubules were assembled at 37°C as described in the previous section, except that no rhodamine tubulin was added. After varying times of assembly, a 4-μl sample was applied to a copper electron microscope grid covered with a holey carbon film. The grid was lightly glow discharged in air before use. Humid air at 35°C was gently blown onto the grid to prevent evaporation and self-cooling of the sample droplet that can lead to microtubule depolymerization (Chrétien and Wade, 1992). The grid was blotted and rapidly plunged into liquid ethane cooled in liquid nitrogen using a guillotine device. Specimens were either stored in liquid nitrogen or were loaded directly into a cryotransfer stage (model 626; Gatan Inc., Pleasanton, CA) and observed in an electron microscope (EM 400; Philips Technologies, Cheshire, CT) equipped with an anticontamination device built in-house. Images were recorded at a nominal magnification of 19,500 under low dose conditions at an under focus of 1–2 μm. The magnification was found to be 18,100 when calibrated under the working conditions by mixing tobacco mosaic virus with some specimens of separate GDP and GMPCPP microtubules.

Image Analysis

Microtubule Populations and Moiré Patterns. A selection was made of micrographs showing microtubule images with clearly visible moiré fringe patterns. These patterns are related to small rotations of the surface lattice that enable different numbers of protofilaments to fit into the microtubule wall. Based on their fringe patterns, individual microtubules can be classified according to the number of protofilaments (Chrétien and Wade, 1991; Wade et al., 1990). The periodicity of the moiré patterns (LN) is related to the number of protofilaments (N), the distance between protofilaments (xp), the rise between monomers in adjacent protofilaments (r), and to the S start helix pitch (Sa), where a is the monomer separation along the protofilaments (Fig. 1):

$$LN = Nxp/(rN - Sa) \quad (1)$$

A selection was made of micrographs showing microtubule images with clearly visible moiré fringe patterns. The whole area of each micrograph was printed at three times magnification. Microtubules were classed according to their protofilament numbers as identified by their characteristic image contrasts. The total lengths of each type were measured directly on the prints using a map measurer, and the percentages of the complete population were calculated (Table I). Total lengths of 450 and 290 μm were measured, respectively, for GDP and GMPCPP microtubules. The moiré pattern periodicities were measured, using a ruler, on the same prints. By far, the largest number of measurements were made on the majority populations of 14 protofilament microtubules for which more than 350 values were obtained for both assembly conditions.

Computer Analysis. Micrographs were digitized using a CCD camera controlled by IMSTAR software installed on a PC. A 0.1-mm spacing graticule (Graticules Ltd., Tonbridge, England) engraved on glass was overlaid on the micrographs to give a magnification calibration for each digitized image. Image files were transferred to a Silicon Graphics 4D/310 GTX workstation, and all the image manipulations were carried out using SUPRIM software. Subimages of individual microtubule segments were extracted, and where necessary, the microtubule image was set horizontal, straightened, and its background was corrected. Each subimage was floated up to pixel dimensions of $x = 1024$ (horizontal) and $y = 512$ (vertical) before computation of the diffraction intensity (power spectrum). The position of the three-start helix peak on the nominal "40-Å" layer line was measured directly from the displayed power spectrum using a mouse-controlled cursor. The spacing (d) corresponding to the measured layer-line separation (X_m) was obtained for each image by calibration using the separation of the maxima (X_c) arising from the 0.1-mm spacing in the power spectrum of the graticule. For an electron optical magnification (M):

$$d = 0.01\ X_c/MX_m \quad (2)$$

The measured values of d are expected to depend somewhat on the rotation angle of the surface lattice so they should change slightly depending on the moiré period LN. We have checked that this effect is very small compared to the differences in d values that we have found between the GDP and the GMPCPP microtubules. All other things being equal, the d value for the GMPCPP microtubules ($LN \sim 6400$ Å) should be 0.03 Å smaller than for GDP microtubuls ($LN \sim 4600$ Å). This is within the experimental error of the measured d values (see Results).

Results

GMPCPP and GDP Microtubules Have Different Protofilament Skew Angles

Specimens of microtubules polymerized with GTP or the nonhydrolyzable analogue GMPCPP were prepared for electron cryomicroscopy. Microtubules were polymerized in the presence of either of the two nucleotides at 37°C. After varying times of polymerization, a small drop was applied to an electron microscope grid, excess liquid was blotted off, and the grid was rapidly cooled in liquid ethane. The microtubules were observed in vitreous ice by electron cryomicroscopy. Fig. 2 shows microtubules polymerized with GTP

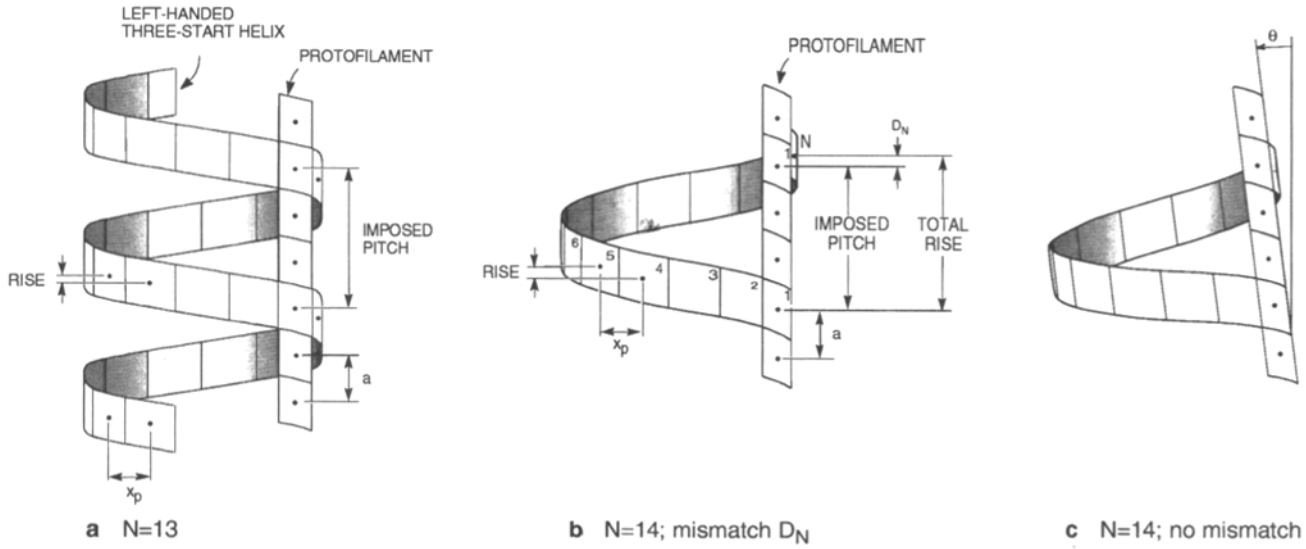

Figure 1. Representation of features of the microtubule surface lattice that follow the surface of a tube. Protofilaments are head-to-tail alignments of the tubulin dimer. These are considered as identical here, and the monomer spacing along the protofilament is *a*. Protofilaments are separated by a distance x_p, and only one protofilament is shown. Each protofilament is shifted upwards (*rise*) with respect to its neighbor so that adjacent monomers follow the left-handed helical path shown. (*a*) $N = 13$. In the canonical 13-protofilament structure, the protofilaments are parallel to axis of the tube, and after one turn, the helix matches onto the reference protofilament at a distance 3 a above its starting position; this is the imposed pitch. (*b*) $N = 14$. The helical path now has a total rise that does not match onto the reference protofilament, and the surface lattice has a mismatch; D_N = *total rise − imposed pitch.* This will occur for any number of protofilaments (N) different to 13. (*c*) The mismatch can be removed by a global rotation of the surface lattice so that the protofilaments are tilted by an angle θ with respect to the microtubule axis.

and with GMPCPP. Each microtubule has two dark edges that enclose a number of lighter striations. These fringes result from the superposition in projection of the protofilaments running along the top and bottom surfaces of the microtubule. The protofilament lattice follows a rotating path around the microtubule (Fig. 1) and therefore forms a moiré pattern in which the fringes are either clear or blurred as the protofilaments on the top and bottom surfaces are periodically superimposed or intercalated (Mandelkow and Mandelkow, 1985; Wade et al., 1990).

We first examined the moiré patterns for microtubules polymerized in the presence of GTP. The patterns fall into clearly defined classes that allow the number of protofilaments in each microtubule to be determined. (Chrétien and Wade, 1991; Wade et al., 1990). The simplest pattern is that of a 13-protofilament microtubule shown in Fig. 2 *a*. It consists of a set of two fringes running along the microtubule for the entire visible length showing that the protofilaments are parallel to the microtubule axis. All the other microtubules show typical moiré patterns in which the fringes appear and disappear at regular intervals because of the rotated protofilaments. We can use the fringe patterns to assign protofilament numbers to the different microtubules: Fig. 2 *b* shows a 14-protofilament microtubule with a repeating pattern of two and then three centered fringes, and Fig. 2 *c* shows a 15-protofilament with a repeating pattern of three off-center fringes. The moiré patterns show that, for the assembly conditions used, a population of 12-, 13-, 14-, and 15-protofilament microtubules is obtained with the 13- and 14-protofilament categories, accounting for 87% of the total (Table I).

We examined the moiré patterns for microtubules polymerized with GMPCPP. Fig. 2 *a* shows a GMPCPP microtubule with two central striations characteristic of a 13-protofilament microtubule. Unlike a 13-protofilament GTP microtubule, the lattice has a twist with a moiré period of 11,370 Å. We examined microtubules with pattern of striations corresponding to 13- (Fig. 2 *a*), 14- (Fig. 2 *b*), and 15- (Fig. 2 *c*) protofilament numbers. We measured the moiré pattern repeat lengths for microtubules with different protofilament numbers. In all cases, these microtubules had a defined moiré pattern that was different from that of microtubule polymerized in the presence of GTP (Table I). Under these conditions, 96% of GMPCPP microtubules had 14 protofilaments (Table I). To confirm that each fringe pattern corresponded to the same number of protofilaments as in GDP microtubules, we measured microtubule width of GMPCPP and GDP microtubules. The width of a microtubule is directly related to the number of protofilaments in the lattice. In all cases, the width measured was that expected for the number of protofilaments (data not shown).

The clearly defined differences in the moiré pattern periodicities of stable GMPCPP and unstable GDP microtubules indicate that the angle of rotation of the protofilament lattice in the two microtubule types is different.

GMPCPP and GDP Microtubules Have Different Subunit Spacing along the Protofilaments

Previous work has suggested that the angle of rotation of the protofilaments lattice should be sensitive to small changes in the size of tubulin subunits in the microtubule or the way that

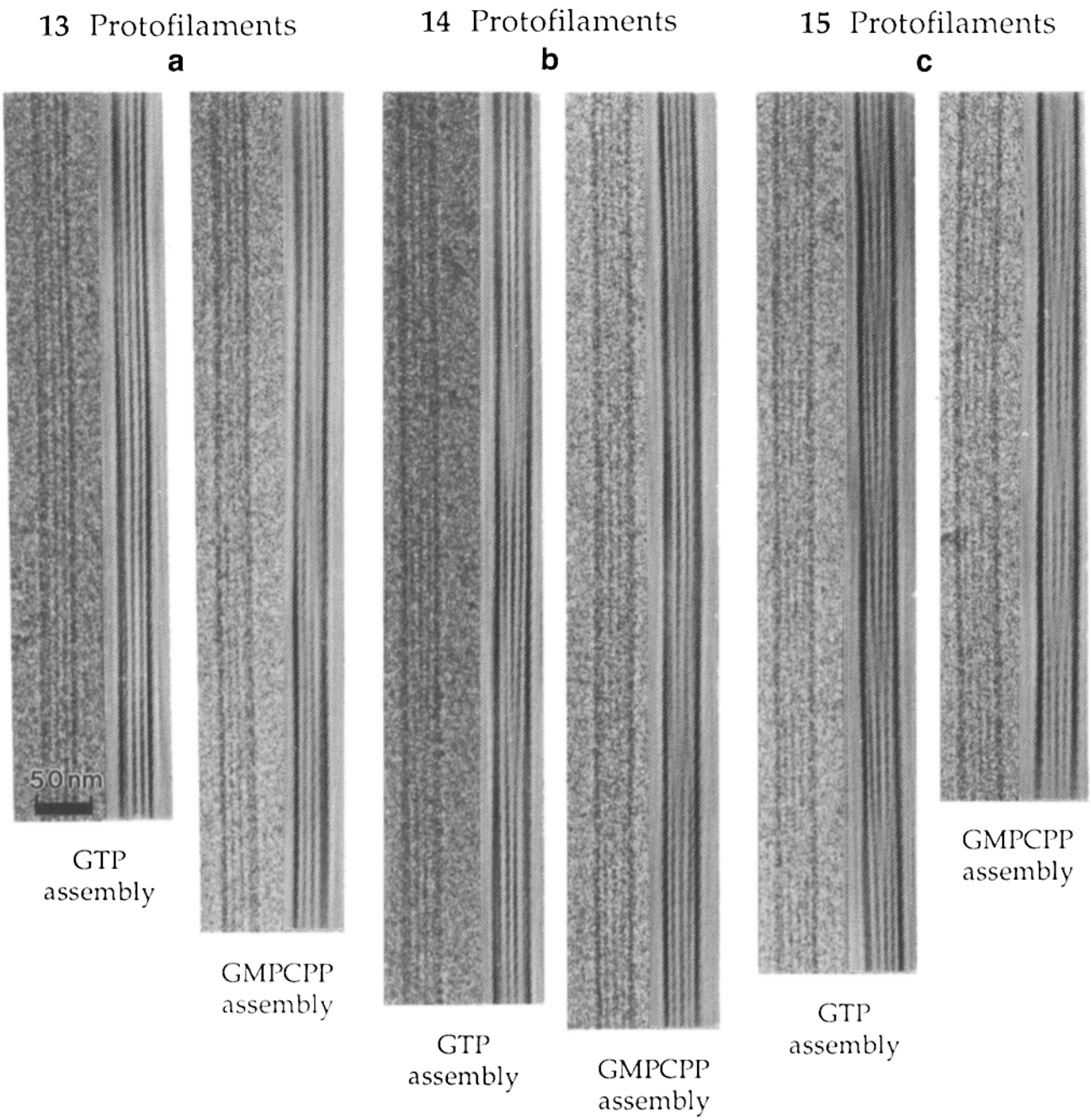

Figure 2. Individual microtubule images with the corresponding computer filtered image. The fringe patterns, more clearly visible in the filtered images, are characteristic of the indicated numbers of protofilaments. For each number of protofilaments, the left panel is the experimental and filtered image of a GDP microtubule and the right panel is the same for a GMPCPP microtubule. Images of microtubules with (*a*) 13 protofilaments, (*b*) 14 protofilaments, and (*c*) 15 protofilaments. Magnification marker corresponds to 500 Å.

subunits in the microtubule interact together (Chrétien and Wade, 1991; Wade et al., 1990). The spacing of tubulin monomers in the protofilament can be examined by looking at optical diffraction from laser light shining on a microtubule. Because the tubulin subunits in a microtubule polymerize head to tail with a repeating structure, the microtubule wall can be imagined as a very fine grating. Light shining on a microtubule will diffract as it passes through microtubule, with a pattern characteristic of the spacing of the tubulin monomers along the protofilament. For microtubules, this repeat can be seen every 40 Å, corresponding to the length of 1 monomer (Erickson, 1974; Amos and Klug, 1974).

We examined a large set of micrographs by optical and computer "diffraction," and we selected microtubule images that gave significant intensity on the nominally 40-Å layerline. To unambiguously measure this spacing, we used TMV as an in situ calibration of the electron optical magnification (Finch, 1964). The diffraction pattern for microtubules polymerized in the presence of GTP showed a clear layer-

Table I. Populations and Moiré Repeat Distances for GDP and GMPCPP Microtubules

	Number of protofilaments			
	12	13	14	15
Theory				
Fringe pattern	2/0/1 Centered	2 or 0 Offset	2/0/3 Centered	3/0/3 Offset
L_N (moiré repeat)	3,448 Å	None	4023 Å	2155 Å
GTP assembly				
Population	2.8%	38.3%	49%	9.9%
L_N	3,861 ± 500 Å	None	4,662 ± 384 Å	2,334 ± 172 Å
GMPCPP assembly				
Population	0.2%	3.1%	96%	0.7%
L_N	3,088 Å (one value)	11,370 Å	6,396 ± 970 Å	2,720 Å (one value)

line at 40.5 ± 0.2 Å, an average of 25 measurements. We then examined the diffraction pattern of microtubules polymerized with GMPCPP. Optical diffraction of the GMPCPP microtubules showed a shift in the position of the layer-line to 43 ± 0.2 Å, an average of 20 measurements. Fig. 3 *a* shows the distribution of the layer-line distances measured on the computed diffraction patterns from these calibration grids for separate assembly in the presence of GTP and of GMPCPP.

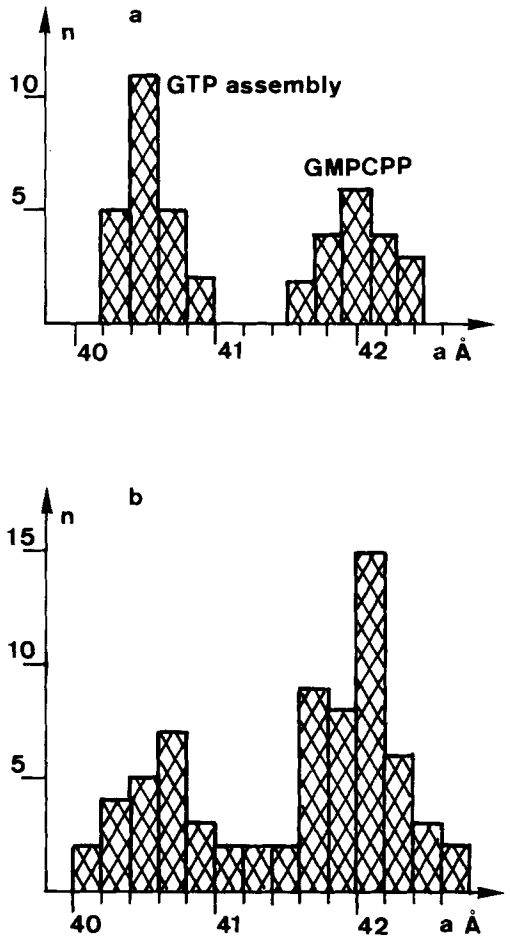

Figure 3. Histograms showing numbers of measurements (*n*) of layer-line spacings for micrographs of microtubules (*a*) assembled separately in the presence of GTP and GMPCPP. The magnification of the micrographs was calibrated using TMV in situ. (*b*) Micrographs of specimens containing both types of microtubule. In this case, the magnification of the images was scaled against the calibrated measurements.

To be sure that the differences between the microtubules prepared with the two nucleotides were not caused by subtle differences in the preparation or observation conditions, we wished to carry out the electron microscopy with both types of microtubule on the same grid. To make these mixed specimens, we decided to grow GDP microtubules from existing GMPCPP microtubules. We established the conditions for obtaining roughly equal lengths of GDP and GMPCPP microtubules using fluorescence light microscopy (Hyman et al., 1991). First, the GMPCPP microtubules were grown for 1 h at a tubulin concentration of 0.3 mg/ml, and then these microtubules were mixed into a final concentration of 3 mg/ml of rhodamine-GTP-tubulin. Under these conditions, the GTP-tubulin was found to grow only from the ends of the existing GMPCPP microtubules. To ensure that the new microtubules were polymerized from GTP-tubulin, we arranged the nucleotide concentrations so that GTP was 10-fold more concentrated than GMPCPP. Since GMPCPP competes with GTP at ~25% efficiency (Hyman et al., 1992), we assumed that there would be a 40:1 ratio of GTP/GMPCPP tubulin in the newly grown microtubules. At different time points, the lengths of the GDP segments was examined by fluorescence of the rhodamine probe. This allowed us to establish conditions giving roughly equal lengths of both types of microtubule. We prepared these segmented microtubules in the absence of rhodamine tubulin for electron microscopy.

Fig. 4 *a* shows two 14-protofilament microtubules from a mixed GMPCPP and GDP grid, one with a moiré pattern corresponding to a GDP microtubule (*A*) and the other with a pattern corresponding to a GMPCPP microtubule (*B*). The computed diffraction intensities are shown side by side in Fig. 4 *b*. We measured the diffraction peak positions for random selections of microtubule images in the micrographs obtained from the "mixed" grids. The population of the corresponding spacing is shown in Fig. 3 *b*. As can be seen, the layer-line positions fall into two classes corresponding to the average 40.5- and 42-Å spacing seen in Fig. 3 *a* for separately polymerized GDP or GMPCPP microtubules.

We wondered how the GMPCPP and GDP lattices would affect each other at the transition between them. Fig. 5 shows a 14-protofilament microtubule with a transition from a

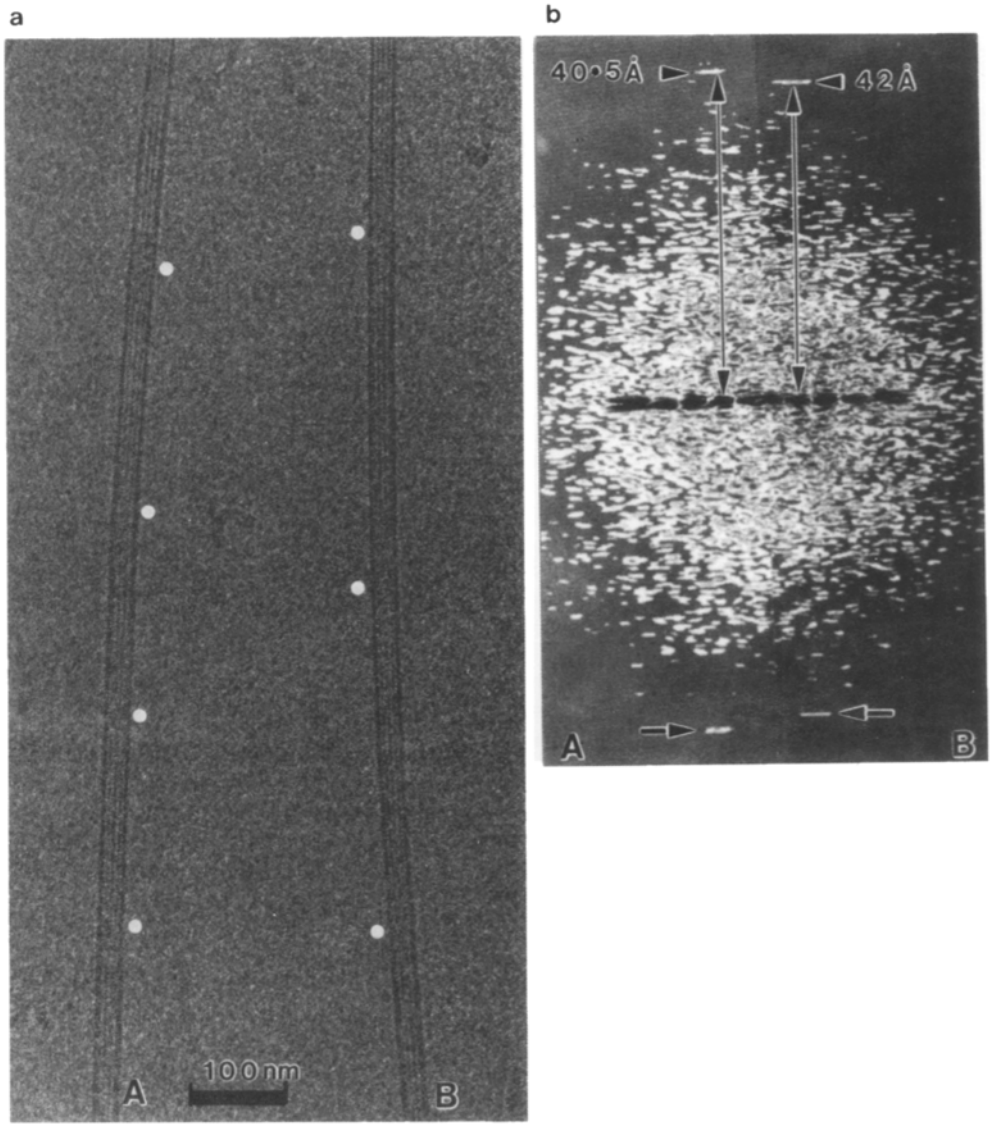

Figure 4. Mixed assembly to give GDP and GMPCPP microtubules on the same grids. (*a*) Two 14-protofilament microtubules showing moiré pattern repeats typical of (*A*) GDP microtubules and (*B*) of GMPCPP microtubules. Bar corresponds to 1,000 Å. (*b*) Arrows denote the computed diffraction intensities of *A* and *B* with the layer-line intensities. The different level of the equivalent peaks indicates a difference in the spacing of the tubulin subunits along the protofilaments in (*A*) GDP microtubules, spacing = 40.5 Å; and in (*B*) GMPCPP microtubules, spacing = 42 Å.

moiré pattern corresponding to a GDP microtubule (*A*) to one corresponding to a GMPCPP microtubule (*B*). The layer-line spacing, computed for short sections of microtubule segments, is plotted as a function of position along the microtubule. An abrupt change in spacing is found at the transition between the moiré patterns typical of GDP and GMPCPP microtubules. The computations were made for sections corresponding to ~20 dimers in length, so the change in the microtubule lattice clearly takes place over a shorter distance than this. We have attempted to estimate the length of the transition by taking smaller and smaller windows. Our results so far suggest that the change occurs within <10 dimer lengths, showing that we can detect the layer-line position accurately using diffraction from a total of ~140 dimers.

Finally, we checked the accumulated set of measurements of moiré repeat distances (L) and diffraction patterns in micrographs of mixed grids and of separate calibrated grids to see whether the values of L are related to the measured layer-line spacing (Fig. 1, *a*). Fig. 6 *b* shows unequivocally that these two parameters are related, and the separate clouds indicate that the GDP and the GMPCPP microtubules form two distinct classes. The close agreement between the diffraction patterns obtained from the mixed and from the separate calibration grids show that we are measuring real differences in the position of the 40Å layer-line.

The GMPCPP Microtubule Lattice Accommodates the Difference in Monomer Spacing by a Change in the Skew Angle of the Protofilaments

We used the lattice accommodation theory (Chrétien and Wade, 1991; Wade et al., 1990) to give a quantitative estimate of how changes in the size of the tubulin monomer affect the moiré pattern periodicity (see Fig. 1). This model provides a geometric relationship between the parameters that determine the lattice structure, such as protofilament number and subunit size, as well as moiré pattern length. We calculated how the moiré period would be influenced by independently modifying three parameters related to tubulin monomer spacing: (*a*) the protofilament separation, which depends on the monomer "width" (X_p; Fig. 1 *a*); (*b*) the monomer rise from protofilament to protofilament, related to the lateral contacts between monomers (*rise*; Fig. 1 *a*);

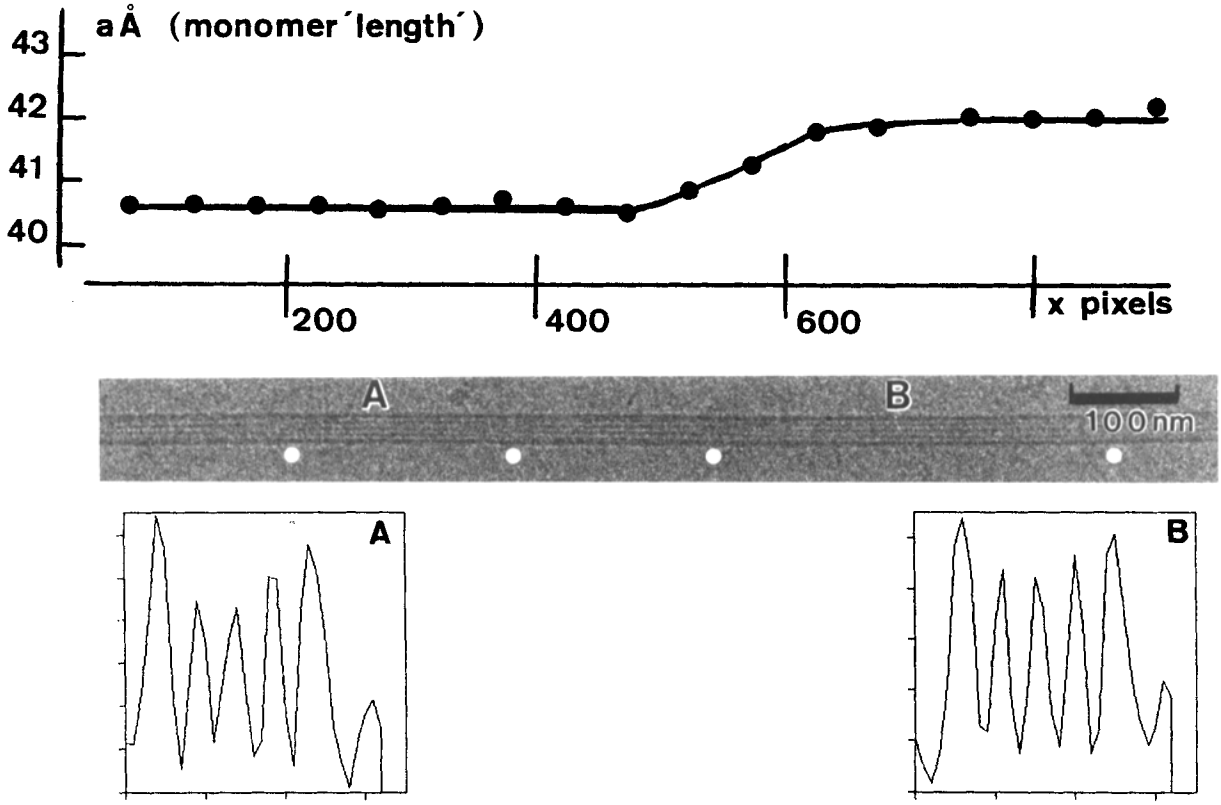

Figure 5. 14-Protofilament microtubule in a mixed assembly experiment; the blurred segments of the moiré pattern are marked by the white spots. There is a transition from the moiré pattern spacing typical of a GDP microtubule, region A, to that of a GMPCPP microtubule, region B. The graph above the image shows the monomer "length," *a*, i.e., the layer-line spacings measured on the computed diffraction patterns from segments 150 pixels long (i.e., ~20 dimers) for the indicated positions along the microtubule. Intensity profiles shown for sections across the image at positions *A* and *B* indicate that the microtubule has the same width on either side of the transition. Magnification marker, 1,000 Å.

and (*c*) the subunit spacing along protofilaments, related to the monomer "length" (*a*; Fig. 1 *b*). Fig. 6 *a* shows the theoretical relationships between changes in these parameters and the moiré pattern length. Of these test calculations, only the situation (*c*), a change in subunit spacing along the microtubule, predicts the experimental data. In Fig. 6 *b*, the curve represents the theoretical relationship between the size of the monomer spacing along the protofilaments and the moiré periodicity, which the symbols represent the observed subunit size for different moiré periodicities. The position of this line with respect to the experimental points indicates that the a 1.5-Å change in subunit spacing will give the observed moiré pattern changes in GMPCPP microtubules. This implies that the rotation of the protofilament lattice is most probably induced by modifications in the subunit spacing along the protofilaments.

Discussion

GMPCPP-Tubulin Subunits Have Different Conformation from GDP-Tubulin Subunits in the Microtubule Lattice

Our results imply that tubulin subunits in microtubules polymerized with a GMPCPP lattice have a different conformation to tubulin subunits in microtubules with a GDP lattice. The 1.5-Å difference, represents a ~4% change in the position of the 40-Å layer line and corresponds to a lengthwise change in the spacing of the tubulin subunits along the protofilaments. Since we were able to record images of GDP and GMPCPP microtubules in the same micrographs, artifacts such as slight magnification changes from grid to grid (or within the same specimen if the grid is distorted) can be discarded. 4% is well within the measurement accuracy of the diffraction patterns, showing that we have measured a real change in the subunit spacing. The implied change in shape of the tubulin subunits cannot be interpreted in any detail from the diffraction data. However, we have also observed that incorporation of GMPCPP in the microtubule lattice changes the moiré pattern in the microtubule images. Because moiré patterns are long range patterns, they magnify small changes in protofilament skew angles. Interpretation of the moiré patterns using the lattice accommodation model suggests that the subunits increase in length while the lateral contacts between the subunits remain unchanged. The lateral contacts situated on the shallow three-start helix are probably the regions involved in lateral stabilization of the protofilaments in the microtubule lattice. Since GMPCPP microtubules are stable compared with GDP microtubules (Hyman et al., 1992), this suggests that the conformational

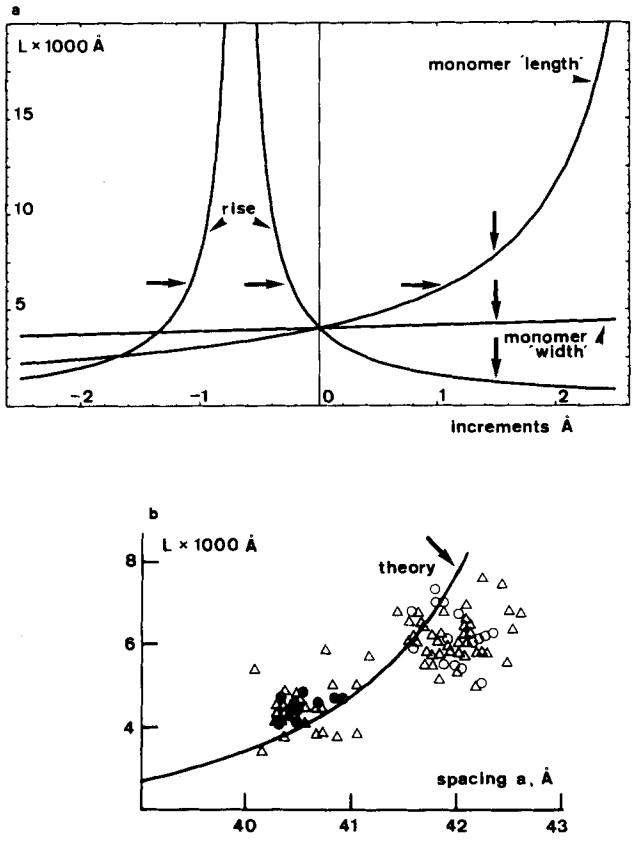

Figure 6. (*a*) Predicted change from the lattice accommodation theory of the repeat length of the moiré pattern as a function of changes in the protofilament spacing (related to the width of the monomer), the rise between subunits of adjacent protofilaments and the length of the monomer. (*b*) Showing the relationship between the layer-line spacing, a, and the moiré pattern repeat distances, L, for individual microtubules in the mixed specimens (*open triangles*), for the calibration grids with separate assembly of GDP (*full circles*), and GMPCPP microtubules (*open circles*). The theoretical dependence of L on the separation a between the subunits along the protofilaments was calculated using Eq. 1 with $N = 14$, $x_p = 51.5$ Å, $r = 9.346$ Å, and $S = 3$. The value of r corresponds to the rise for the GDP microtubules.

change is involved in the stabilization of microtubules against depolymerization.

The Role of GTP Hydrolysis in Microtubule Destabilization

The dynamic properties of microtubules polymerized with GMPCPP and other GTP analogues show clearly that GTP hydrolysis has evolved to destabilize the microtubule lattice (Arai and Kaziro, 1976; Hyman et al., 1992; Mejillano et al., 1990; Penningroth and Kirschner, 1977; Seckler et al., 1990; Weisenberg and Deery, 1976). Observations of microtubules during growing and shrinking phases have shown that protofilaments at the end of the microtubule change their morphology during the transition from growth to shrinkage. During growth, the end of the microtubule is probably a sheet of protofilaments, and the wall of the microtubule closes into a tube behind this growing sheet (Simon and Salmon, 1990; Chrétien, D., S. Fuller, and E. Karsenti, manuscript submitted for publication). The protofilaments in the sheet have a gentle curve. By contrast, when microtubules shrink, the protofilaments loose contact with each other and roll up into oligomers (Mandelkow et al., 1991). The chemical energy that allows this large structural change is released during GTP hydrolysis. However, the small difference in conformation seen between the GDP and the GMPCPP lattices, which we assume to correspond to the hydrolyzed and nonhydrolyzed forms, suggests that much of the energy released by GTP hydrolysis is stored in the lattice and is released during microtubule disassembly as part of the large conformational change that takes place as protofilaments disconnect and roll up into circular forms.

One possibility is that GTP hydrolysis weakens the interprotofilament interactions. For instance, an unhydrolyzed cap of GTP subunits at the end of the microtubule could stabilize the end of the lattice by strong interprotofilament contacts, and protofilament contacts in the microtubule could weaken after GTP hydrolysis. Although we cannot rule out the weakening of interprotofilament interactions by GTP hydrolysis, our results suggest that it is unlikely. Rather, there is only a subtle difference between the structure of the microtubule before and after hydrolysis, and modeling suggests that this difference does not affect the interprotofilament contacts.

How, then, does GTP hydrolysis destabilize the microtubule lattice? During depolymerization, protofilaments tend to unwind from the microtubule (Mandelkow et al., 1991; Simon and Salmon, 1990). Such a tendency to unwind would act in opposition to interprotofilament contacts that stabilize the microtubule. Any increase in protofilament curvature would, therefore, tend to destabilize microtubules. We propose that increase in protofilament curvature is the change that takes place when the GTP is hydrolyzed, an idea previously suggested on the basis of studies that examined the shape of the depolymerization products of microtubules (Melki et al., 1989). Our diffraction results suggest that upon GTP hydrolysis, the tubulin subunit spacing along the protofilaments shortens. We speculate that the tubulin monomers could curl up slightly into a kidney bean–like shape and appear shorter. Thus, the chemical energy is transmitted to mechanical strain in the lattice that we have seen indirectly as the change in protofilament twist in the microtubule. This mechanical strain tends to unwind the protofilaments, since the string of aligned beans tends to bend outwards to follow the curvature of the individual beans. As the energy is released, protofilament unwinding will propagate from the microtubule ends inwards along the microtubule.

The relative timing of the two reactions of microtubule assembly and GTP hydrolysis are still unknown when microtubules polymerize in the presence of GTP. All attempts to verify the GTP cap model by biochemical means have failed so far (e.g., O'Brien et al., 1987). Most of the problems come from detecting the signal of unhydrolyzed GTP in the microtubule lattice above the noise of unhydrolyzed GTP free in solution. We have shown that as few as 140 dimers, and maybe less, are required to see the 40-Å layer-line, and therefore should be able to detect GTP-tubulin in the microtubule lattice over lengths less than ~800 Å. Since we have been able to detect very small changes (~1.5 Å) in the subunit–subunit interactions that may be involved in the stabilization of the microtubule via GTP hydrolysis, we may

be able to visualize small regions of unhydrolyzed GTP in the microtubule lattice and thus probe the timing and position of GTP hydrolysis during microtubule polymerization.

The authors would like to thank Linda Amos for the first observations on optical diffraction on GMPCPP microtubules, as well as Eric Karsenti, Michael Glotzer, Steve Fuller, and Werner Kulbrandt for helpful comments during the course of these studies and critical reading of the manuscript.

Received for publication 18 July 1994 and in revised form 7 October 1994.

References

Amos, L., and A. Klug. 1974. Arrangements of subunits in flagellar microtubules. *J. Cell. Sci.* 14:523–549.

Arai, T., and Y. Kaziro. 1976. Effect of guanine nucleotide on the assembly of brain microtubules: ability of guanylyl imidodiphosphate to replace GTP in promoting the polymerization of microtubules in vitro. *Biochem. Biophys. Res. Commun.* 69:369–376.

Carlier, M. F. 1989. Role of nucleotide hydrolysis in the dynamics of actin filaments and microtubules. *Int. Rev. Cytol.* 115:139–170.

Cassimeris, L., S. Inoue, and E. D. Salmon. 1988. Microtubule dynamics in the chromosomal spindle fiber: analysis by fluorescence and high-resolution polarization microscopy. *Cell Motil. Cytoskeleton.* 10:185–196.

Chen, Y. D., and T. L. Hill. 1985. Monte Carlo study of the GTP cap in a five-start helix model of a microtubule. *Proc. Natl. Acad. Sci. USA.* 82:1131–1135.

Chrétien, D., and R. H. Wade. 1991. New data on the microtubule surface lattice. *Biol. Cell.* 71:161–174.

Chrétien, D., F. Metoz, E. Karsenti, and R.H. Wade. 1992. Lattice defects in microtubules: protofilament numbers vary within microtubules. *J. Cell Biol.* 117:1031–1040.

Erickson, H. P. 1974. Microtubule surface lattice and subunit structure and observations on reassembly. *J. Cell Biol.* 60:153–167.

Erickson, H. P., and E. T. O'Brien. 1992. Microtubule dynamic instability and GTP hydrolysis. *Annu. Rev. Biophys. Biomol. Struct.* 21:145–166.

Finch, J. T. 1964. Resolution of the substructure of tobacco mosaic virus in the electron microscope. *J. Mol. Biol.* 8:872–874.

Gelfand, V. I., and A. D. Bershadsky. 1991. Microtubule dynamics: mechanism, regulation and function. *Annu. Rev. Cell Biol.* 7:93–116.

Howard, J., and A. A. Hyman. 1993. Preparation of marked microtubules for the assay of the polarity of microtubule-based motors by fluorescence microscopy. *Methods Cell Biol.* 39:105–113.

Hyman, A. A., D. Drexel, D. Kellog, S. Salser, K. Sawin, P. Steffen, L. Wordeman, and T. J. Mitchison. 1991. Preparation of modified tubulins. *Methods Enzymol.* 196:478–485.

Hyman, A. A., S. Salser, D. Drechsel, N. Unwin, and T. J. Mitchison. 1992. The role of GTP hydrolysis in microtubule dynamics: information from a slowly hydrolyseable analogue GMPCPP. *Mol. Cell. Biol.* 3:1155–1167.

Kirschner, M. W. 1978. Microtubule assembly and nucleation. *Int. Rev. Cytol.* 54:1–71.

Kirschner, M. W., and T. J. Mitchison. 1986. Beyond self assembly: from microtubules to morphogenesis. *Cell.* 45:329–342.

Mandelkow, E. M., and E. Mandelkow. 1985. Unstained microtubules studies by cryoelectron microscopy: substructure, supertwist and disassembly. *J. Mol. Biol.* 181:123–135.

Mandelkow, E. M., E. Mandelkow, and R. Milligan. 1991. Microtubule dynamics and microtubule caps: a time-resolved cryoelectron microscopy study. *J. Cell Biol.* 114:977–992.

Mejillano, M. R., J. S. Barton, J. P. Nath, and R. H. Himes. 1990. GTP analogues interact with the tubulin exchangeable site during assembly and upon binding. *Biochemistry.* 29:1208–1216.

Melki, R., M. F. Carlier, D. Pantaloni, and S. N. Timasheff. 1989. Cold depolymerization of microtubules to double rings: geometric stabilization of assemblies. *Biochemistry.* 28:9143–9152.

Mitchison, T. J., and T. J. Kirschner. 1984. Dynamic instability of microtubule growth. 312:237–242.

O'Brien, E. T., W. A. Voter, and H. P. Erickson. 1987. GTP hydrolysis during microtubule assembly. *Biochemistry.* 26:4148–4156.

Penningroth, S. M., and M. W. Kirschner. 1977. Nucleotide binding and phosphorylation in microtubule assembly in vitro. *J. Mol. Biol.* 115:643–673.

Penningroth, S. M., and M. W. Kirschner. 1978. Nucleotide specificity in microtubule assembly in vitro. *Biochemistry.* 17:734–740.

Purich, D. L., and D. Kristoffersen. 1984. Microtubule assembly: a review of progress, principles, and perspectives. *Adv. Protein Chem.* 36:133–212.

Seckler, R., G. M. Wu, and S. N. Timasheff. 1990. Interactions of tubulin with guanylyl-(beta-gamma-methylene)diphosphonate. Formation and assembly of a stochiometric complex. *J. Biol. Chem.* 265:7655–7661.

Simon, J. R., and E. D. Salmon. 1990. The structure of microtubule ends during the elongation and shortening phases of dynamic instability examined by negative stain electron microscopy. *J. Cell Sci.* 96:571–582.

Stewart, R. J., K. W. Farrel, and L. Wilson. 1990. Role of GTP hydrolysis in microtubule polymerization: evidence for a coupled hydrolysis mechanism. *Biochemistry.* 29:6489–6498.

Wade, R. H., D. Chrétien and D. Job. 1990. Characterization of microtubules protofilament numbers. *J. Mol. Biol.* 212:775–786.

Walker, R. A., E. T. O'Brien, N. K. Pryer, M. F. Sobeiro, W. A. Voter, H. P. Erickson, and E. D. Salmon. 1988. Dynamic instability of individual microtubules analyzed by video light microscopy: rate constants and transition frequencies. *J. Cell Biol.* 107:1437–1448.

Weisenberg, R. C., and W. J. Deery. 1976. Role of nucleotide hydrolysis in microtubule assembly. *Nature (Lond.).* 263:792–793.